Technical note: Use of $PM_{2.5}$ to CO ratio as an indicator of wildfire smoke in urban areas

Daniel A. Jaffe[1,2], Brendan Schnieder[3] and Daniel Inouye[3]

[1]School of STEM, University of Washington, Bothell, WA, 98011, USA
[2]Department of Atmospheric Sciences, University of Washington, Seattle, WA, 98195, USA
[3]Washoe County Health District, Air Quality Management Division, Reno, NV, USA

Correspondence to: Daniel A. Jaffe (djaffe@uw.edu)

Abstract. Wildfires and the resulting smoke are an increasing problem in many regions of the world. However, identifying the contribution of smoke to pollutant loadings in urban regions can be challenging at low concentrations due to the presence of the usual array of anthropogenic pollutants. Here we propose a method using the difference in $PM_{2.5}$ to CO emission ratios between smoke and typical urban pollution. For temperate wildfires, the mean emission ratio of $PM_{2.5}$ to CO is in the range of 0.14-0.18 g/g, whereas typical urban emissions have a $PM_{2.5}$ to CO emissions ratio that is lower by a factor of 2-20. This gives rise to the possibility of using this ratio as an indicator of wildfire smoke.. We use observations at a regulatory surface monitoring site in Sparks, NV, for the period of May-September 2018-2021. There were many smoke-influenced periods from numerous California wildfires that burned during this period. Using a $PM_{2.5}$/CO threshold of 30.0 µg m^{-3} ppm^{-1}, we can split the observations into smoke-influenced and no-smoke periods. We then develop a Monte Carlo simulation, tuned to local conditions, to derive a set of $PM_{2.5}$/CO values that can be used to identify smoke influence in urban areas. From the simulation, we find that a smoke enhancement ratio of 140 µg m^{-3} ppm^{-1} best fits the observations, which is significantly lower than the ratio observed in fresh smoke plumes (e.g. 200-300 µg m^{-3} ppm^{-1}). The most likely explanation for this difference is loss of $PM_{2.5}$ during dilution and transport to warmer surface layers. We find that the $PM_{2.5}$/CO ratio in urban areas is an excellent indicator of smoke and should prove to be useful to identify biomass burning influence on the policy relevant concentrations of both $PM_{2.5}$ and O_3. Using the results of our Monte Carlo simulation, this ratio can also quantify the influence of smoke on urban $PM_{2.5}$.

1. Introduction

In the U.S., smoke has become an increasingly challenging problem due to a significant increase in the area burned by wildfires (Zhuang et al 2021; Kalashnikov et al 2022; McClure and Jaffe 2018). Data from the National Interagency Fire Center (www.nifc.gov) showed that between the early 1980s and 2021, the decadal average annual area burned by wildfires in the U.S. increased by almost a factor of 3, from 1.1 to 3.0 million ha per year. Multiple factors were responsible for this increase, including climate change, increasing human ignitions and past forest management (Jaffe et al 2020).

Primary emissions from fires include fine particulate matter with diameter of less than 2.5 µm ($PM_{2.5}$), carbon monoxide (CO), nitrogen oxides ($NO_x=NO+NO_2$), and hundreds of volatile organic compounds (VOCs), which include many toxic and hazardous air pollutants (Akagi et al 2011; Permar et al 2021). Furthermore, atmospheric chemistry leads to O_3 and other secondary products. The cumulative impact of these emissions has substantial health implications (e.g., Ebi et al 2021; O'Dell
35 et al 2020; 2021; Gan et al 2020; Doubleday 2020; Sorenson et al 2021).

Smoke at the surface can originate from nearby or distant fires (e.g., DeBell et al 2004; Jaffe et al 2004; Teakles et al 2017; Rogers et al 2020). Satellites can provide an exceptional geospatial view of fires and the occurrence and transport of smoke (e.g., Duncan et al 2014; Jaffe et al 2020; Kahn 2020; O'Neill et al 2021; Holloway et al 2021). But with very few exceptions, satellite data provide little to no vertical information directly. Modeling of smoke transport and exposure is challenging for a
40 number of reasons, including uncertainties in emissions, plume injection heights and model resolution (Lu et al 2016; O'Neill et al 2021; Ye et al 2021). It is possible to measure unique smoke tracers , such as acetonitrile (CH_3CN) (Singh et al 2012; Chandra et al 2020), but these measurements are not routinely performed at surface sites and also have some anthropogenic sources (Huangfu et al 2021).

Wildfire emissions are chemically distinct from industrial and vehicle emissions in having very high $PM_{2.5}$ emissions per unit
45 of fuel burned. Table 1 shows emissions ratios (ERs) of $PM_{2.5}$/CO, expressed on a g/g basis along with observed and calculated NERs normalized enhancement ratios (NERs, $\Delta PM_{2.5}/\Delta CO$), for smoke and non-smoke sources. The $PM_{2.5}$/CO ERs from temperate wildfires are at least a factor of 1.9 greater than the same ER for anthropogenic emissions. Comparing the $PM_{2.5}$/CO ERs from wildfires with vehicle emissions, we see that wildfires emit 15-19 times the amount of $PM_{2.5}$ per unit of CO emitted. Using these ERs we can estimate normalized enhancement ratios (NER, $\Delta PM_{2.5}/\Delta CO$), assuming no chemical or physical loss
50 of either species (also shown in Table 1). Observed NERs will reflect not only the emissions, but also chemical and physical processing, plus any background contribution. The observed NERs in urban areas with no smoke (21-66, mean of 37 µg m^{-3} ppm^{-1}) are much closer to the estimated NERs for vehicle emissions, which is reasonable given these are usually the largest source of both $PM_{2.5}$ and CO in urban areas.

The observed smoke NERs appear to fall into two groups. At the surface, mean smoke NERs are in the range of 103-128 µg
55 m^{-3} ppm^{-1}, whereas in fresh plumes aloft, the mean values are 201-339 µg m^{-3} ppm^{-1}. The values aloft are much closer to the mean NER (220 µg m^{-3} ppm^{-1}) calculated from the most recent compilation of ERs for temperate forests (Andreae et al 2019). Selimovic et al (2019; 2020) noted that the $PM_{2.5}$/CO NER in ground-level smoke is about half of that observed from aircraft or free tropospheric observations. This was most likely caused by a reduction in aerosol mass from evaporation of organic aerosols due to higher surface temperatures and greater downstream dilution. These past observations present a fairly
60 consistent picture showing that $PM_{2.5}$/CO NER for surface smoke is about 3-4 times greater than the NER for typical urban observations in the absence of smoke, based on the values given in Laing et al (2017).

Table 1. Emission ratios (ERs) and observed NERs for non-smoke and smoke conditions. ERs are converted into NERs using a pressure of 1 atmosphere and temperature of 273K (STP). This calculation assumes no loss of either $PM_{2.5}$ or CO. For observed ERs and NERs, the study mean is given and the range (if reported) is shown in parentheses.

	$PM_{2.5}$/CO E.R. (g/g)	$PM_{2.5}$/CO NER ($\mu g\ m^{-3}$ ppm^{-1})
Non-smoke emissions and observed NERs		
US industrial and mobile emissions (excludes wildfires and residential wood combustion)[1]	0.076	95
U.S. Mobile sources only[1]	0.009	11
Observed NERs in urban areas with no smoke[2]		37 (21-66)
Smoke emissions and observed NERs		
Temperate wildfires ERs[3]	.142	177
Temperate wildfires ERs[4]	.176 (.07-.57)	220 (87-712)
Observed smoke NERs in urban areas[2]		128 (57-228)
Observed smoke NERs, surface sites[5]		103 (120-156)
Fresh plumes, high elevation site[6]		258 (66-377)
Fresh plumes, high elevation site and aircraft data[7]		299 (170-630)
Fresh plumes, aircraft data[8]		201 (80-400)
Fresh plumes, aircraft data[9]		339 (21—492)

[1]Data from the EPA's 2017 National Emission Inventory (EPA 2022).
[2]Data from Laing et al 2017.
[3]Data from Akagi et al 2011.
[4]Data from Anderea 2019.
[5]Data from Selimovic et al 2020.
[6]Data from Briggs et al 2016. Scattering values are reported at STP and converted to $PM_{2.5}$ using a dry mass scattering coefficient of 3.5 m^2g^{-2}
[7]Data from Collier et al 2016. This value includes refractory PM_1. Values are adjusted to STP.
[8]Data from Garofolo et al 2019. This value includes only the organic, non-refractory PM_1 fraction, however this is likely more than 90% of total $PM_{2.5}$ mass. Values are adjusted to STP.
[9]Data from Kleinman et al 2020. This value includes only the non-refractory PM_1 mass. Values are adjusted to STP.

The very different $PM_{2.5}$ to CO NERs for typical urban air and smoke events suggest that the observed ratios can be used to derive the smoke contribution to surface $PM_{2.5}$ concentrations. (Laing et al 2017; Xiu et al 2022). To examine this hypothesis, we used data from a monitoring site in Sparks, NV, near Reno, a region that has been heavily influenced by smoke in the past several years due to the large number and extent of California wildfires. Data from this region were used to examine the role of high $PM_{2.5}$ exposure from smoke on COVID-19 incidence (Kiser et al 2021). From the Sparks, NV, observations, we developed a quantitative model using a Monte Carlo simulation (Baez and Tweed 2013) that provides a range of probabilistic results that can be compared to observations. We found that this method appears to reasonably quantify the smoke contribution in an urban area.

2. Methods and data sources

For this analysis, we use daily mean $PM_{2.5}$ and CO concentrations for May-September 2018-2021 from the Sparks, NV, air quality monitoring site (EPA AQS identification #320311005) near Reno, NV, that is operated by the Washoe (NV) County Health District, Air Quality Management Division. The site uses instruments and standards that are consistent with the national EPA requirements (40 CFR Part 58) and report data into the EPA's national Air Quality System (AQS). The Sparks site has near-continuous measurements of $PM_{2.5}$, CO and O_3. We used data for May–September 2018–2021 to avoid complications with sources from residential wood combustion. Data were obtained from the EPA AirData site (https://www.epa.gov/outdoor-air-quality-data), except for 2021 data, which were obtained from AirNow-Tech, a web-based data resource operated for the U.S. EPA (https://www.airnowtech.org/). Instrumentation at the Sparks site included a MetOne model 1020 Beta Attenuation Monitor (BAM) for $PM_{2.5}$, a Teledyne API model 300 EU non-dispersive IR monitor for CO and a Teledyne API model T400 UV O_3 analyser. These instruments have stated detection limits (DLs) of 1 $\mu g\ m^{-3}$, 20 ppb and 0.4 ppb, respectively. Because there were some zero and very low values, $PM_{2.5}$ concentrations less than the DL were set to 1 $\mu g\ m^{-3}$. This impacted less than 2% of the dataset. No below DL values were reported for the CO or O_3 data. As an indication of overhead smoke, we used the daily smoke polygon product from the NOAA Hazard Mapping System-Fire and Smoke Product (hereafter simply HMS). The smoke polygon product is created by expert image analysts that digitize smoke plume extent a few times per day based on analysis of GOES-16 and GOES-17 ABI True Color Imagery available during daylight hours. More details on HMS are in Rolph et al (2009) and Kaulfus et al (2017). We note that HMS can sometimes miss thin smoke plumes, especially in the presence of clouds (Buysse et al 2019). Buysse et al (2019) found that there is enhanced surface $PM_{2.5}$ on 30-70% of the days with overhead HMS smoke, depending on the location.

3. Results

Figure 1 shows one example of the HMS smoke product for the Loyalton fire on Aug. 16, 2020, which was about 35-45 km from the Sparks monitoring site. This fire started on 8/14/2020 and burned for approximately one month. In total, this fire burned approximately 20,000 ha in the Tahoe and Humboldt-Toiyabe National Forests. On 8/16/2020, the daily mean $PM_{2.5}$ and CO concentrations were 38 $\mu g\ m^{-3}$ and 0.43 ppm at the Sparks, NV monitoring site. Washoe County is located due east of the California-Nevada border, so smoke from many fires in California is often transported to the Sparks monitor. Table 2 shows data for the number of days that exceeded the U.S. National Ambient Air Quality Standards (NAAQS) for $PM_{2.5}$ (2006 24-hour standard, daily mean of 35 $\mu g\ m^{-3}$) and O_3 (2015 8-hour O_3 standard, maximum daily 8-hour mean of 0.070 ppm) for the Sparks monitoring site, along with the annual area burned in California. While 2020 was the highest year on record for the area burned in CA for the past 2 decades, 2021 was the second highest year and had a greater number of days in Reno that exceeded the NAAQS. Note that 2019 was a particularly low fire year in CA, and there were no exceedances of either the daily $PM_{2.5}$ or O_3 NAAQS at the Sparks monitoring site. Overall, for this time period (May-September 2018-2021), 200 out

of 612 days had overhead HMS smoke at the Sparks monitoring location.   The PM$_{2.5}$/CO smoke criteria is discussed later in this section.

Table 2: California area burned, overhead HMS smoke days, and days over the U.S. National Ambient Air Quality Standard at Sparks, NV, for PM$_{2.5}$ (daily mean of 35 µg m^{-3}) and O$_3$ (70 ppb, 8 hour average).   The smoke criteria (indicated by *) uses a PM$_{2.5}$ /CO ratio of 30.0 µg m^{-3} ppm^{-1}, as discussed later in text.

	2018	2019	2020	2021
California area burned (Ha)	7.4E5	1.0E5	1.7E6	1.1E6
Sparks Overhead HMS smoke (days)	51	11	52	86
Sparks smoke days*	42	30	81	67
Identified smoke days with no HMS identification	13	25	20	15
PM$_{2.5}$ exceedance days	6	0	19	22
PM$_{2.5}$ exceedance days with smoke*	6	0	19	22
O$_3$ exceedance days	10	0	5	13
O$_3$ exceedance days with smoke*	8	0	5	11

Figure 2 shows the daily PM$_{2.5}$ vs CO concentrations for May-Sept 2018-2021, segregated for smoke vs non-smoke conditions. The data are segregated using (1) the HMS smoke product and (2) a PM$_{2.5}$/CO ratio $\geq$ 30.0 . The value of 30.0 was chosen based, in part, on the work of Laing et al (2017) and on evaluation of likely smoke influence.   We found the slopes and correlations were not strongly influenced by the choice of PM$_{2.5}$/CO ratio. For example, using a ratio of <20, <30, <40 and <50 we get slopes of 16.5, 18.0, 23.4 and 33.9 µg m^{-3} per ppm, an increasing pattern as would be expected. We found that smoke influence can be observed on some days at a PM$_{2.5}$/CO ratio as low as 32. An example of this is 8/5/2018, when extensive and heavy smoke blanketed most of California, Nevada and other western states.   PM$_{2.5}$ and CO concentrations at Sparks were 22 µg m^{-3} and 0.68 ppm, respectively, for a PM$_{2.5}$/CO ratio of 32.   The relatively low ratio implies significant mixing of this smoke event with air containing a lower ratio, but the high PM$_{2.5}$ concentrations and widespread smoke are consistent with a significant smoke influence on that day.   Using the PM$_{2.5}$/CO ratio to segregate the data, we found an improved correlation of PM$_{2.5}$ and CO in the lower range of ratios, compared with using the HMS as an indicator (Figure 2).

Table 3 summarizes the results. There are 612 days in the analysis. 200 have a positive HMS smoke identification and 220 have PM$_{2.5}$/CO ratios$\geq$30. There are 73 days with PM$_{2.5}$/CO ratios$\geq$30 but without a positive HMS smoke identification and 53 days that have a positive HMS smoke identification, but a low PM$_{2.5}$/CO ratio (<30). The first category (high PM$_{2.5}$/CO ratio, but no HMS smoke) can be considered a false negative (smoke is present but not detected by HMS), whereas the second category (HMS smoke present, but low PM$_{2.5}$/CO ratios) can be considered a false positive. While there is relatively little difference between the mean and SD of the smoke-influenced and non-smoke data, the improved correlation suggests that the PM$_{2.5}$/CO ratio is a better way to segregate the dataset. The exact choice of PM$_{2.5}$/CO ratio depends on the certainty required. This is discussed in more detail using a Monte Carlo simulation, as described below.

Table 3. Sparks daily PM₂.₅ and CO data for May-September 2018-2021, segregated by the PM₂.₅/CO ratio and by overhead HMS smoke.

	PM$_{2.5}$/CO <30.0 (no smoke)	PM$_{2.5}$/CO ≥30.0 (smoke-influenced)
Count	392	220
Mean PM$_{2.5}$ (µg m^{-3})	4.7	25.4
Std. Dev. (µg m^{-3})	1.9	28.6
Count of days with HMS =1	53	147
	HMS=0 (no smoke)	HMS=1 (smoke-influenced)
Count	412	200
Mean PM$_{2.5}$ (µg m^{-3})	5.0	26.9
Std. Dev. (µg m^{-3})	2.0	29.6
Count of days with PM$_{2.5}$/CO ≥30.0	73	147

We used the PM$_{2.5}$ and CO data to develop a Monte Carlo simulation of the PM$_{2.5}$/CO ratio for Reno using the following relationships:

$$\text{PM}_{2.5}\ (\mu g\ m^{-3}) = \text{Urban PM}_{2.5} + \text{Smoke PM}_{2.5} + \text{background PM}_{2.5} = 10^{\alpha} + 10^{\beta} + 2\ \mu g/m^3 \quad (1)$$

$$\text{CO (ppm)} = \text{Urban PM}_{2.5}/\text{R}_{\text{urban}} + \text{Smoke PM}_{2.5}/\text{R}_{\text{smoke}} + 0.2\ \text{ppm} \quad (2)$$

Where R$_{\text{urban}}$ and R$_{\text{smoke}}$ are the NERs (ΔPM$_{2.5}$/ΔCO) to represent urban emissions and smoke, respectively. The smoke terms in equations 1 and 2 were non-zero on 1/3 of the days, corresponding to the fractional incidence of HMS smoke. We explored a range of values for R$_{\text{urban}}$ and R$_{\text{smoke}}$ as shown in Table 4. The parameters α and β were used to represent the log-normal distributions for urban PM$_{2.5}$ with, and without, smoke PM$_{2.5}$, respectively. Equations 1 and 2 include a background contribution to represent natural, biogenic, and intercontinental sources of PM$_{2.5}$ and CO. The background concentrations were set to 2 µg m^{-3} for PM$_{2.5}$ and 0.2 ppm for CO. These background values were estimated based on observations from 2019, a low fire year, from a rural continental site (West Yellowstone, MT AQS #300310017) and a marine background site (Cheeka Peak, WA, AQS #530090013). During the May-Sept 2019 period the West Yellowstone mean values for PM$_{2.5}$ and CO were 2.5 µg m^{-3} and 0.24 ppm, whereas the Cheeka Peak site the mean values were 2.1 µg m^{-3} and .08 ppm. Median values were very similar at both sites. We note that PM$_{2.5}$ concentrations were similar at both sites, whereas CO was higher at the continental site. Given that Sparks, NV is a continental/inland location, the West Yellowstone, MT concentrations are likely more representative of its background concentrations. We also examined a range of background values for CO (0.1-0.2 ppm) and PM$_{2.5}$ (1-3 µg m^{-3}) and found little influence on the conclusions.

The Monte Carlo simulations estimate a range of observed PM$_{2.5}$ and CO concentrations using Equations 1 and 2. The simulation computes 10,000 concentrations, where α, β, R$_{urban}$ and R$_{smoke}$ are allowed to vary independently with values as defined in Table 4. These values were chosen to be consistent with the mean and S.D. of the non-smoke (α) and smoke (β) datasets, respectively, excluding the contribution from background concentrations. Note that the Monte Carlo simulations
175 are intended to reflect the bulk distributions, so there is no correspondence between an individual day in the simulation with any particular day in the observations.

Table 4. Parameter values used in the Monte Carlo simulations. For the R$_{urban}$ and R$_{smoke}$ parameters, multiple mean values are considered.

	α (unitless)	β (unitless)	R$_{urban}$ (µg m^{-3} ppm^{-1})	R$_{smoke}$ (µg m^{-3} ppm^{-1})
Mean	0.4	1.3	20,40,80	100,140,200 180
Std. Dev.	0.2	0.4	10	20

Figure 3 shows results of the simulation with varying mean values for the R$_{smoke}$ parameter. Even at very high PM$_{2.5}$ concentrations, the observed PM$_{2.5}$/CO ratio never exceeded 125 µg m^{-3} ppm^{-1}. The simulation suggests an optimum R$_{smoke}$
185 value of 140 µg m^{-3} ppm^{-1}. So, consistent with the work of Laing et al (2017) and Selimovic et al (2019; 2020), we found that the best-fit NER values at the surface were much lower than NERs reported for fresh or free tropospheric smoke plumes (200-300 µg m^{-3} ppm^{-1}).

Figure 4 shows the results of the simulations with varying values for the R$_{urban}$ parameter. The best value of R$_{urban}$ was more difficult to discern. At high PM$_{2.5}$ concentrations and PM$_{2.5}$/CO ratios, R$_{urban}$ has very little influence on the simulated values.
190 At the low range of PM$_{2.5}$ concentrations, a value of 20 µg m^{-3} ppm^{-1} is clearly too low, but there is little difference between the other values so it is not clear which value is optimal. This parameter should reflect the primary PM$_{2.5}$ and CO emissions in the area, plus contributions from secondary organic aerosol (e.g., Nault et al 2021). For Washoe County, NV (the county containing Reno and Sparks) the EPA's 2017 National Emissions Inventory gives primary emissions of PM$_{2.5}$ and CO of 1,482 and 55,529 short tons per year, excluding wildfires and residential wood combustion. This corresponds to a PM$_{2.5}$/CO
195 emission ratio of 0.034 g/g or an enhancement ratio of 39 µg m^{-3} ppm^{-1}. Important constraints on using the Monte Carlo approach to discern the urban, non-smoke PM$_{2.5}$/CO NER are limitations on the instrumentation and the impact of background concentrations at low PM$_{2.5}$ and CO concentrations. Nonetheless, we found that using an R$_{urban}$ parameter of either 40 or 80 has little influence on our results at higher PM$_{2.5}$ concentrations. For the rest of this analysis, we used an R$_{smoke}$ value of 140 and an R$_{urban}$ value of 40.

200 Figure 5 shows the fractional smoke contribution to PM$_{2.5}$ vs the PM$_{2.5}$/CO NER from the Monte Carlo simulations. As specified in the model setup, 2/3 of the points have no smoke contribution. These have a mean PM$_{2.5}$/CO value of 17, with a

range of 6-34. As the Monte Carlo simulations represent a probabilistic approach, we can also look at the likelihood that a given set of points has a specific degree of smoke influence. Figure 5 shows the probability that a given set of $PM_{2.5}/CO$ ratios (binned in units of 10) has more than 50% of the $PM_{2.5}$ due to smoke. So, starting with the $PM_{2.5}/CO$ bin of 30-40, we have a very high probability (0.85) that more than 50% of the $PM_{2.5}$ mass is due to smoke and at a bin of 40-50 we have near certainty (0.993) that more than 50% of the $PM_{2.5}$ mass is due to smoke.

We can use the information in Figure 5 to evaluate the likelihood that smoke contributed to the days with high $PM_{2.5}$ or O_3, as shown in Table 2. The years 2018, 2020 and 2021 all had a significant number of exceedances days (over the NAAQS), whereas the low fire year of 2019 had none. Using a $PM_{2.5}/CO$ value of 30.0 which, based on the Monte Carlo simulation, implies that smoke contributes more than half of the total $PM_{2.5}$ on 85% of days. Even using a smoke criteria of $PM_{2.5}/CO$ of 45, we found no change in the number of smoke-influenced days. Not surprisingly, the $PM_{2.5}/CO$ criteria identified all of the $PM_{2.5}$ exceedance days as smoke influenced, using either smoke criteria (35 or 45). For O_3, the results show that 24 out of the 28 exceedance days were smoke influenced, using either criteria. While the $PM_{2.5}/CO$ ratio can quantitatively estimate the fraction of $PM_{2.5}$ due to smoke (e.g. Figure 5), we note that this approach cannot provide a quantitative estimate of the smoke contribution to the O_3 levels. Other tools would be needed to quantify the smoke contribution to the MDA8 O_3 values (e.g., Ninneman and Jaffe 2021; Jaffe 2021; Gong et al 2017). Nonetheless, the results shown in Table 2 demonstrate that the $PM_{2.5}/CO$ ratio can identify days with a strong smoke signature.

4. Summary

The large difference in $PM_{2.5}/CO$ emission ratios between typical urban pollution and wildfire smoke gives rise to very different observed NERs in urban areas for non-smoke and smoke-influenced conditions. We used $PM_{2.5}$ and CO data for May through September, when residential wood combustion is minimal, to develop a Monte Carlo simulation of the resulting ratios. We find that the Monte Carlo simulation that includes both smoke and non-smoke NERs can accurately reproduce the observed NERs and provides a measure of smoke influence in an urban area. The model supports earlier work that found the $PM_{2.5}/CO$ NER in biomass burning influenced plumes at surface sites is approximately half of that observed in fresh emissions and in cooler environments. This likely is caused by loss of $PM_{2.5}$ mass during transport due to dilution and warmer temperatures at surface sites. For the Sparks, NV monitoring site we found that at a $PM_{2.5}/CO$ ratio of 35 µg m^{-3} ppm^{-1} biomass burning contributed more than half of the total $PM_{2.5}$ on 85% of days. To apply the Monte Carlo simulation at other sites requires that the parameters in Table 4 be adjusted to fit the local data. The R_{urban} parameter would need to be adjusted based on local emissions and observations and the α and β parameters would need to be fit based on the observed non-smoke and smoke concentrations, respectively.

This analysis demonstrates that it is possible to identify wildfire smoke at the surface based on commonly measured air pollutants with high confidence. While satellite data can also identify smoke influence, these have both high false positive and negative rates, meaning that many days identified by satellite products as having overhead smoke show little or no

influence at the surface and many days that have smoke at the surface are missed by the HMS product.. We conclude that the

235 observed PM$_{2.5}$/CO ratio provides a more robust signal of surface smoke in urban areas and with no false positives.

References

Akagi, S. K., Yokelson, R. J., Wiedinmyer, C., Alvarado, M. J., Reid, J. S., Karl, T., Crounse, J. D., and Wennberg, P. O.:
Emission factors for open and domestic biomass burning for use in atmospheric models, Atmos. Chem. Phys., 11,
240 4039-4072, https://doi.org/10.5194/acp-11-4039-2011, 2011.

Baez, J.C. and Tweed, D. Monte Carlo methods in Climate Science. Math Horizons, November 2013. (available at:
https://www.maa.org/sites/default/files/pdf/horizons/baeztweed_nov13.pdf, accessed May 2022.)

Brey, S. J., Ruminski, M., Atwood, S. A., and Fischer, E. V.: Connecting smoke plumes to sources using Hazard Mapping
System (HMS) smoke and fire location data over North America, Atmos. Chem. Phys., 18, 1745-1761,
245 https://doi.org/10.5194/acp-18-1745-2018, 2018.

Briggs, N. L., Jaffe, D. A., Gao, H., Hee, J. R., Baylon, P. M., Zhang, Q., Zhou, S., Collier, S. C., Sampson, P. D., and Cary,
R. A.: Particulate matter, ozone, and nitrogen species in aged wildfire plumes observed at the Mount Bachelor
Observatory. Aerosol Air Qual. Res 16, 3075–3087, https://doi.org/10.4209/aaqr.2016.03.0120, 2016.

Buysse, C. E., Kaulfus, A., Nair, U., and Jaffe, D. A.: Relationships between particulate matter, ozone, and nitrogen oxides
250 during urban smoke events in the western US, Environ. Sci. Technol., 53, 12519-12528,
https://doi.org/10.1021/acs.est.9b05241, 2019.

Chandra, B. P., McClure, C. D., Mulligan, J., and Jaffe, D. A.: Optimization of a method for the detection of biomass-
burning relevant VOCs in urban areas using thermal desorption gas chromatography mass spectrometry,
Atmosphere, 11, 276, https://doi.org/10.3390/atmos11030276, 2020.

255 DeBell, L. J., Talbot, R. W., Dibb, J. E., Munger, J. W., Fischer, E. V., and Frolking, S. E.: A major regional air pollution
event in the northeastern United States caused by extensive forest fires in Quebec, Canada, J. Geophys. Res.-
Atmos., 109, https://doi.org/10.1029/2004jd004840, 2004.

Doubleday, A., Schulte, J., Sheppard, L., Kadlec, M., Dhammapala, R., Fox, J., and Busch Isaksen, T.: Mortality associated
with wildfire smoke exposure in Washington State, 2006–2017: a case-crossover study, Environ. Health, 19, 4,
260 https://doi.org/10.1186/s12940-020-0559-2, 2020.

Duncan, B. N., Prados, A. I., Lamsal, L. N., Liu, Y., Streets, D. G., Gupta, P., Hilsenrath, E., Kahn, R. A., Nielsen, J. E.,
Beyersdorf, A. J., Burton, S. P., Fiore, A. M., Fishman, J., Henze, D. K., Hostetler, C. A., Krotkov, N. A., Lee, P.,
Lin, M., Pawson, S., Pfister, G., Pickering, K. E., Pierce, R. B., Yoshida, Y., and Ziemba, L. D.: Satellite data of
atmospheric pollution for U.S. air quality applications: Examples of applications, summary of data end-user
265 resources, answers to FAQs, and common mistakes to avoid, Atmos. Environ., 94, 647-662,
https://doi.org/10.1016/j.atmosenv.2014.05.061, 2014.

Ebi, K. L., Vanos, J., Baldwin, J. W., Bell, J. E., Hondula, D. M., Errett, N. A., Hayes, K., Reid, C. E., Saha, S., Spector, J.,
and Berry, P.: Extreme weather and climate change: Population health and health system implications, Annu. Rev.
Publ. Health, 42, 293-315, https://doi.org/10.1146/annurev-publhealth-012420-105026, 2021.

270   Gan, R. W., Liu, J., Ford, B., O'Dell, K., Vaidyanathan, A., Wilson, A., Volckens, J., Pfister, G., Fischer, E. V., Pierce, J. R., and Magzamen, S.: The association between wildfire smoke exposure and asthma-specific medical care utilization in Oregon during the 2013 wildfire season, J. Expo, Sci. Environ. Epidemiol., 30, 618-628, https://doi.org/10.1038/s41370-020-0210-x, 2020.

Garofalo, L. A., Pothier, M. A., Levin, E. J. T., Campos, T., Kreidenweis, S. M., and Farmer, D. K.: Emission and evolution
275   of submicron organic aerosol in smoke from wildfires in the western United States, ACS Earth Space Chem., 3, 1237-1247, https://doi.org/10.1021/acsearthspacechem.9b00125, 2019.

Gong, X., Kaulfus A., Nair, U., and Jaffe, D. A.: Quantifying O_3 impacts in urban areas due to wildfires using a Generalized Additive Model. Environ. Sci. Tech., 55, 13216-13223, https://doi.org/10.1021/acs.est.7b03130, 2017.Hadley, O., Cutler, A., Schumaker, R., and Bond, R.: Wildfires and wood stoves: Woodsmoke toxicity and chemical
280   characterization study in the north-western United States, Atmos. Environ., 253, 118347, https://doi.org/10.1016/j.atmosenv.2021.118347, 2021.

Holloway, T., Miller, D., Anenberg, S., Diao, M., Duncan, B., Fiore, A. M., Henze, D. K., Hess, J., Kinney, P. L., Liu, Y., Neu, J. L., O'Neill, S. M., Odman, M. T., Pierce, R. B., Russell, A. G., Tong, D., West, J. J., and Zondlo, M. A.: Satellite monitoring for air quality and health, Annu. Rev. Biomed. Data Sci., 4, 417-447,
285   https://doi.org/10.1146/annurev-biodatasci-110920-093120, 2021.

Huangfu, Y., Yuan, B., Wang, S., Wu, C., He, X., Qi, J., et al.: Revisiting acetonitrile as tracer of biomass burning in anthropogenic-influenced environments. Geophys. Res. Lett., 48, e2020GL092322. https://doi.org/10.1029/2020GL092322, 2021.

Jaffe D. Evaluation of Ozone Patterns and Trends in 8 Major Metropolitan Areas in the U.S. Final project report for CRC
290   Project A-124, Coordinating Research Council, Alpharetta, GA, March 2021. Available at: http://crcao.org/wp-content/uploads/2021/04/CRC-Project-A-124-Final-Report_Mar2021.pdf.

Jaffe, D. A., Bertschi, I., Jaegle, L., Novelli, P., Reid, J. S., Tanimoto, H., Vingarzan, R., and Westphal, D. L.: Long-range transport of Siberian biomass burning emissions and impact on surface ozone in western North America, Geophys. Res. Lett., 31, L16106–L16106, https://doi.org/10.1029/2004GL020093, 2004.

295   Jaffe, D. A., O'Neill, S. M., Larkin, N. K., Holder, A. L., Peterson, D. L., Halofsky, J. E., and Rappold, A. G.: Wildfire and prescribed burning impacts on air quality in the United States, J. Air Waste Manage. Assoc., 70, 583-615, https://doi.org/10.1080/10962247.2020.1749731, 2020.

Kahn, R.: A global perspective on wildfires, Eos, 101, https://doi.org/10.1029/2020EO138260, 2020.

Kalashnikov, D. A., Schnell, J. L., Abatzoglou, J. T., Swain, D. L., and Singh, D.: Increasing co-occurrence of fine
300   particulate matter and ground-level ozone extremes in the western United States, Science Advances, 8, eabi9386, https://doi.org/10.1126/sciadv.abi9386, 2022.

Kaulfus, A. S., Nair, U., Jaffe, D., Christopher, S. A., and Goodrick, S.: Biomass burning smoke climatology of the United States: implications for particulate matter air quality, Environ. Sci. Technol., 51, 11731-11741, https://doi.org/10.1021/acs.est.7b03292, 2017.

305   Kiser, D., Elhanan, G., Metcalf, W. J. , Schneider B., and Grzymski J. J. SARS-CoV-2 test positivity rate in Reno, Nevada: association with PM2.5 during the 2020 wildfire smoke events in the western United States. J. Expo. Sci. Environ. Epidemiol., 31, 797–803, https://doi.org/10.1038/s41370-021-00366-w, 2021.

Kleinman, L. I., Sedlacek III, A. J., Adachi, K., Buseck, P. R., Collier, S., Dubey, M. K., Hodshire, A. L., Lewis, E., Onasch, T. B., Pierce, J. R., Shilling, J., Springston, S. R., Wang, J., Zhang, Q., Zhou, S., and Yokelson, R. J.: Rapid
310   evolution of aerosol particles and their optical properties downwind of wildfires in the western US, Atmos. Chem. Phys., 20, 13319–13341, https://doi.org/10.5194/acp-20-13319-2020, 2020.

Kotchenruther, R. A.: Source apportionment of $PM_{2.5}$ at multiple Northwest U.S. sites: Assessing regional winter wood smoke impacts from residential wood combustion, Atmos. Environ., 142, 210-219, https://doi.org/10.1016/j.atmosenv.2016.07.048, 2016.

315 Laing, J. R., Jaffe, D. A., Slavens, A. P., Li, W. T., and Wang, W. X.: Can ΔPM2.5/ΔCO and ΔNOy/ΔCO enhancement ratios be used to characterize the influence of wildfire smoke in urban areas?, Aerosol Air Qual. Res., 17, 2413-2423, https://doi.org/10.4209/aaqr.2017.02.0069, 2017.

Laing, J. R., and Jaffe, D. A.: Wildfires are causing extreme PM concentrations in the western United States, EM, July, 2019.

320 Lu, X., Zhang, L., Yue, X., Zhang, J. C., Jaffe, D. A., Stohl, A., Zhao, Y. H., and Shao, J. Y.: Wildfire influences on the variability and trend of summer surface ozone in the mountainous western United States, Atmos. Chem. Phys., 16, 14687-14702, https://doi.org/10.5194/acp-16-14687-2016, 2016.

Magzamen, S., Gan, R. W., Liu, J., O'Dell, K., Ford, B., Berg, K., Bol, K., Wilson, A., Fischer, E. V., and Pierce, J. R.: Differential cardiopulmonary health impacts of local and long-range transport of wildfire smoke, GeoHealth, 5, 325 e2020GH000330, https://doi.org/10.1029/2020GH000330, 2021.

McClure, C. D., and Jaffe, D. A.: US particulate matter air quality improves except in wildfire-prone areas, P. Natl. Acad. Sci. USA, 115, 7901-7906, https://doi.org/10.1073/pnas.1804353115, 2018.

Nault, B. A. et al: Secondary organic aerosols from anthropogenic volatile organic compounds contribute substantially to air pollution mortality, Atmos. Chem. Phys., 21, 11201–11224, https://doi.org/10.5194/acp-21-11201-2021, 2021.

330 Ninneman, M., and Jaffe, D. A.: The impact of wildfire smoke on ozone production in an urban area: Insights from field observations and photochemical box modeling. Atmos. Environ., 267, 118764, doi: 10.1016/j.atmosenv.2021.118764, 2021.

O'Dell, K., Hornbrook, R. S., Permar, W., Levin, E. J. T., Garofalo, L. A., Apel, E. C., Blake, N. J., Jarnot, A., Pothier, M. A., Farmer, D. K., Hu, L., Campos, T., Ford, B., Pierce, J. R., and Fischer, E. V.: Hazardous air pollutants in fresh 335 and aged western US wildfire smoke and implications for long-term exposure, Environ. Sci. Technol., 54, 11838-11847, https://doi.org/10.1021/acs.est.0c04497, 2020.

O'Dell, K., Bilsback, K., Ford, B., Martenies, S. E., Magzamen, S., Fischer, E. V., and Pierce, J. R.: Estimated mortality and morbidity attributable to smoke plumes in the United States: not just a western US problem, GeoHealth, 5, e2021GH000457, https://doi.org/10.1029/2021GH000457, 2021.

340 O'Neill, S. M., Diao, M., Raffuse, S., Al-Hamdan, M., Barik, M., Jia, Y., Reid, S., Zou, Y., Tong, D., West, J. J., Wilkins, J., Marsha, A., Freedman, F., Vargo, J., Larkin, N. K., Alvarado, E., and Loesche, P.: A multi-analysis approach for estimating regional health impacts from the 2017 Northern California wildfires, J. Air Waste Manage. Assoc., 71, 791-814, https://doi.org/10.1080/10962247.2021.1891994, 2021.

Permar, W., Wang, Q., Selimovic, V., Wielgasz, C., Yokelson, R. J., Hornbrook, R. S., Hills, A. J., Apel, E. C., Ku, I.-T., 345 Zhou, Y., Sive, B. C., Sullivan, A. P., Collett Jr, J. L., Campos, T. L., Palm, B. B., Peng, Q., Thornton, J. A., Garofalo, L. A., Farmer, D. K., Kreidenweis, S. M., Levin, E. J. T., DeMott, P. J., Flocke, F., Fischer, E. V., and Hu, L.: Emissions of trace organic gases from western U.S. wildfires based on WE-CAN aircraft measurements, J. Geophys. Res.-Atmos., 126, e2020JD033838, https://doi.org/10.1029/2020JD033838, 2021.

Rogers, H. M., Ditto, J. C., and Gentner, D. R.: Evidence for impacts on surface-level air quality in the northeastern US from 350 long-distance transport of smoke from North American fires during the Long Island Sound Tropospheric Ozone Study (LISTOS) 2018, Atmos. Chem. Phys., 20, 671-682, https://doi.org/10.5194/acp-20-671-2020, 2020.

Rolph, G. D., Draxler, R. R., Stein, A. F., Taylor, A., Ruminski, M. G., Kondragunta, S., Zeng, J., Huang, H. C., Manikin, G., McQueen, J. T., and Davidson, P. M.: Description and verification of the NOAA Smoke Forecasting System: the 2007 fire season, Weather Forecast., 24, 361-378, https://doi.org/10.1175/2008waf2222165.1, 2009.

Selimovic, V., Yokelson, R. J., McMeeking, G. R., and Coefield, S.: In situ measurements of trace gases, PM, and aerosol optical properties during the 2017 NW US wildfire smoke event, Atmos. Chem. Phys., 19, 3905-3926, https://doi.org/10.5194/acp-19-3905-2019, 2019.

Selimovic, V., Yokelson, R. J., McMeeking, G. R., and Coefield, S.: Aerosol mass and optical properties, smoke influence on O_3, and high NO_3 production rates in a western U.S. city impacted by wildfires, J. Geophys. Res.-Atmos., 125, e2020JD032791, https://doi.org/10.1029/2020JD032791, 2020.

Singh, H. B., Cai, C., Kaduwela, A., Weinheimer, A., and Wisthaler, A.: Interactions of fire emissions and urban pollution over California: Ozone formation and air quality simulations, Atmos. Environ., 56, 45-51, https://doi.org/10.1016/j.atmosenv.2012.03.046, 2012.

Sorensen, C., House, J. A., O'Dell, K., Brey, S. J., Ford, B., Pierce, J. R., Fischer, E. V., Lemery, J., and Crooks, J. L.: Associations between wildfire-related $PM_{2.5}$ and intensive care unit admissions in the United States, 2006–2015, GeoHealth, 5, e2021GH000385, https://doi.org/10.1029/2021GH000385, 2021.

Teakles, A. D., So, R., Ainslie, B., Nissen, R., Schiller, C., Vingarzan, R., McKendry, I., Macdonald, A. M., Jaffe, D. A., Bertram, A. K., Strawbridge, K. B., Leaitch, W. R., Hanna, S., Toom, D., Baik, J., and Huang, L.: Impacts of the July 2012 Siberian fire plume on air quality in the Pacific Northwest, Atmos. Chem. Phys., 17, 2593-2611, https://doi.org/10.5194/acp-17-2593-2017, 2017.

U.S. Environmental Protection Agency (U.S. EPA 2022). 2017 National Emissions Inventory (NEI) Data. https://www.epa.gov/air-emissions-inventories/2017-national-emissions-inventory-nei-data (accessed January 21, 2022).

Xiu, M., Jayaratne, R., Thai, P., Christensen, B., Zing, I., Liu, X., & Morawska, L. Evaluating the applicability of the ratio of PM2. 5 and carbon monoxide as source signatures. *Environmental Pollution*, *306*, 119278, https://doi.org/10.1016/j.envpol.2022.119278, 2022.

Ye, X., Arab, P., Ahmadov, R., James, E., Grell, G. A., Pierce, B., Kumar, A., Makar, P., Chen, J., Davignon, D., Carmichael, G. R., Ferrada, G., McQueen, J., Huang, J., Kumar, R., Emmons, L., Herron-Thorpe, F. L., Parrington, M., Engelen, R., Peuch, V. H., da Silva, A., Soja, A., Gargulinski, E., Wiggins, E., Hair, J. W., Fenn, M., Shingler, T., Kondragunta, S., Lyapustin, A., Wang, Y., Holben, B., Giles, D. M., and Saide, P. E.: Evaluation and intercomparison of wildfire smoke forecasts from multiple modeling systems for the 2019 Williams Flats fire, Atmos. Chem. Phys., 21, 14427-14469, https://doi.org/10.5194/acp-21-14427-2021, 2021.

Zhuang, Y., Fu, R., Santer, B. D., Dickinson, R. E., and Hall, A.: Quantifying contributions of natural variability and anthropogenic forcings on increased fire weather risk over the western United States, P. Natl. Acad. Sci. USA, 118, e2111875118, https://doi.org/10.1073/pnas.2111875118, 2021.
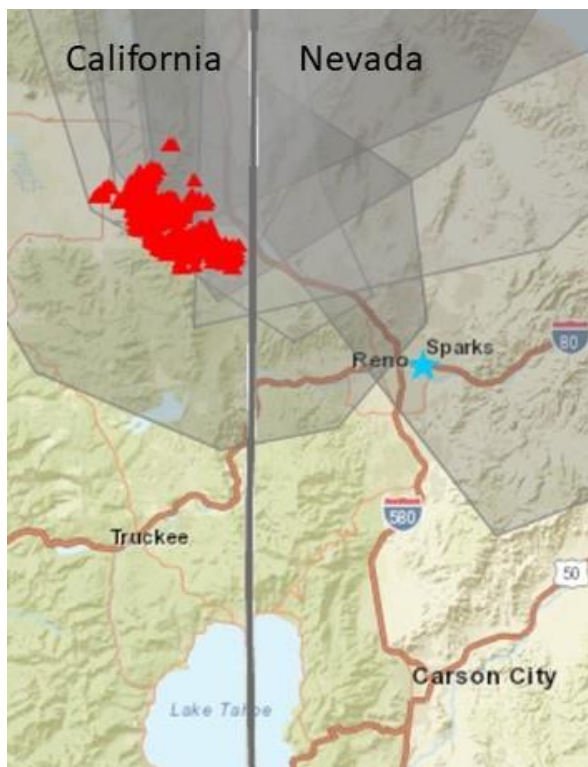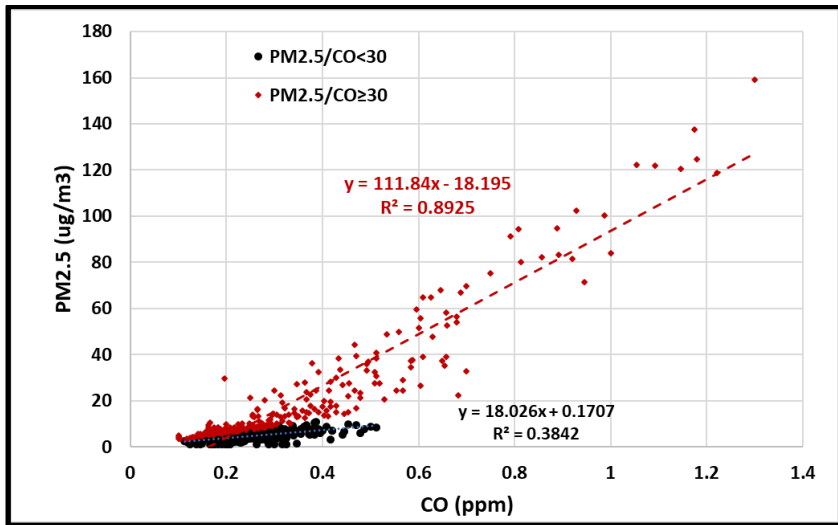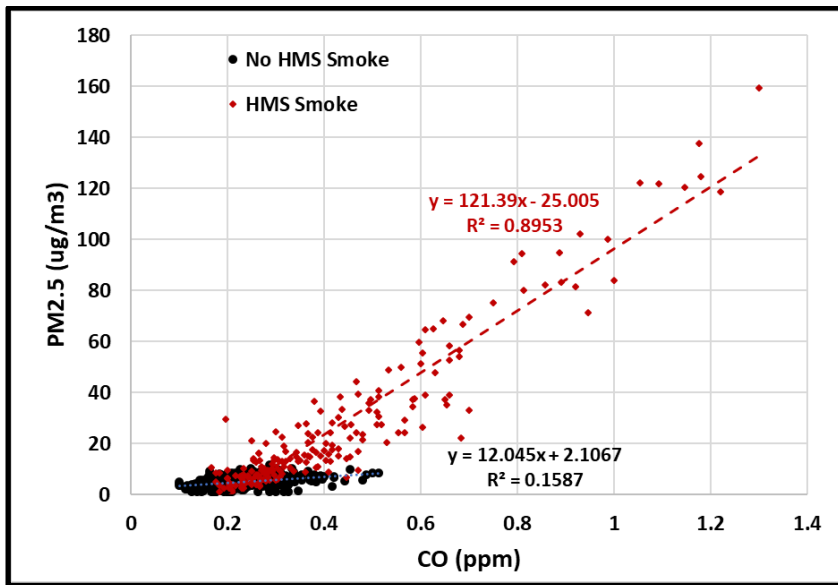
390

Figure 1: NOAA HMS smoke and fire location for Aug. 16, 2020. The Loyalton fire is burning in California near the Nevada border at this time. The blue star shows the location of the Sparks, NV monitoring site, which is approximately 35-45 km from the fire. This map was created from the AirNowTech site (https://www.airnowtech.org/).

395

Figure 2: Observed PM$_{2.5}$ vs CO for May-September data (May 1, 2018-August 31, 2021). Each point is the daily mean of observed values segregated by (top) overhead HMS smoke product or (bottom) PM$_{2.5}$/CO threshold of 30.0 μg m^{-3}/ppm.

400
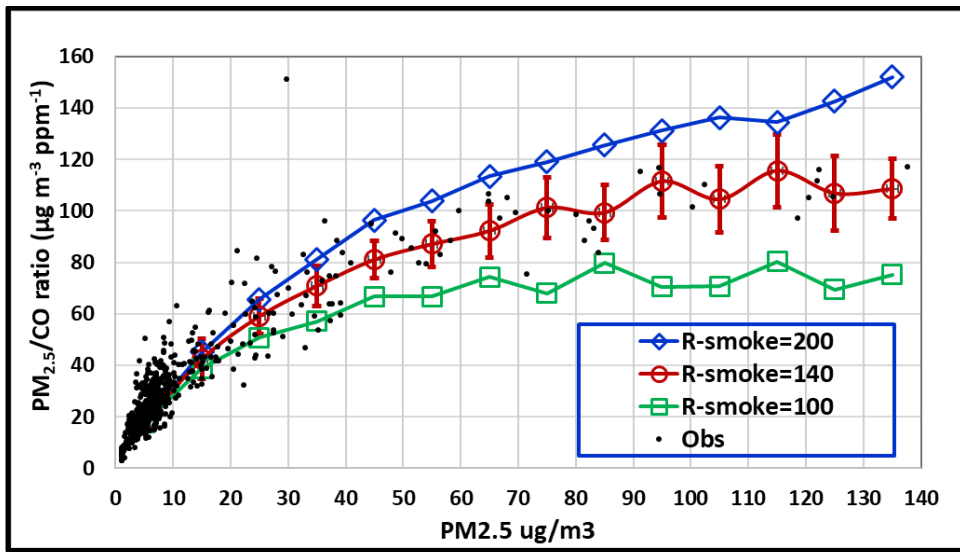
Figure 3. PM$_{2.5}$/CO ratio (μg m^{-3} ppm^{-1}) vs PM$_{2.5}$. The black dots show the observations and the blue diamonds, red circles and green squares show the influence of the R$_{smoke}$ parameter for the urban + smoke simulations. The simulation results are binned in 10 μg m^{-3} intervals centered on the indicated values. For these Monte Carlo simulations, R$_{urban}$ is fixed at 40. Error bars show 1 σ on the middle simulation. One observation is not shown (PM$_{2.5}$/CO ratio of 122 and a PM$_{2.5}$ concentration of 159 μg m^{-3}).
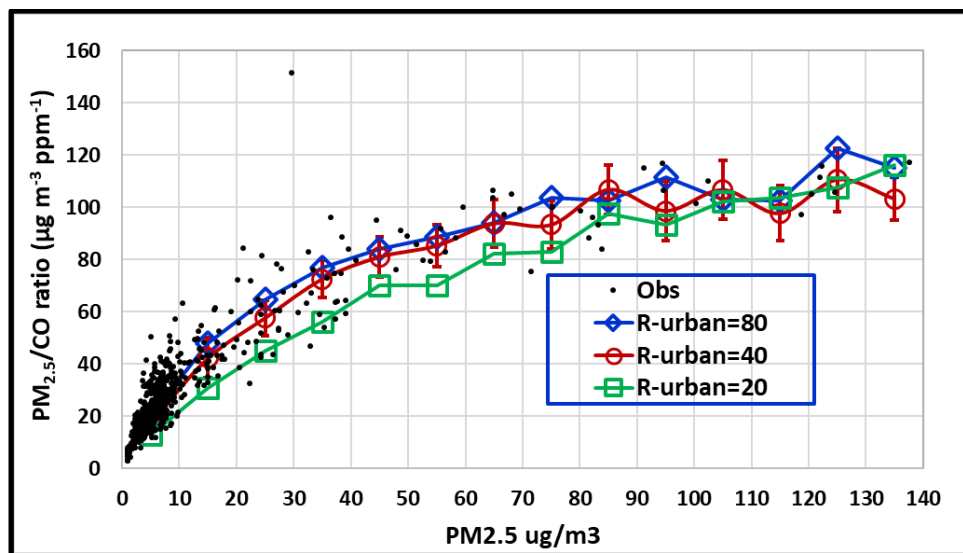
Figure 4. PM$_{2.5}$/CO ratio (µg m^{-3} ppm^{-1}) vs PM$_{2.5}$. The black dots show the observations and the and the blue diamonds, red circles and green squares show the influence of the R$_{urban}$ parameter on the Monte Carlo simulations. The simulation results are binned in 10 µg m^{-3} intervals centered on the indicated values. For these simulations, R$_{smoke}$ is fixed at 140. Error bars show 1 σ on the middle simulation. One observation is not shown (PM$_{2.5}$/CO ratio of 122 and a PM$_{2.5}$ concentration of 159 µg m^{-3}).
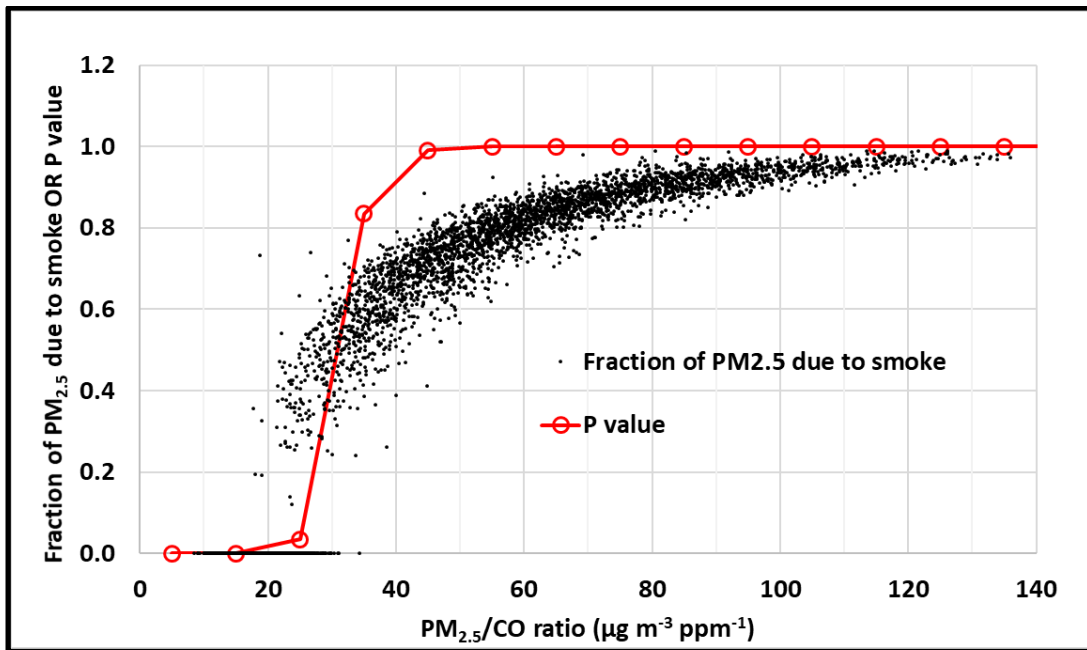
Figure 5. Fraction of PM$_{2.5}$ due to smoke vs the PM$_{2.5}$/CO ratio (µg m^{-3} ppm^{-1}) as calculated from the Monte Carlo simulations. We note that the Monte Carlo simulations give a probabilistic relationship. So, for example, at a PM$_{2.5}$/CO ratio of between 30 and 40, 83% of the points have more than half of the PM$_{2.5}$ due to smoke. The red open circles show the probability that more than 50% of the PM$_{2.5}$ is due to smoke, within each PM$_{2.5}$/CO bin.